INNOVATIVE MECHANICAL ENGINEERING **ISSN 2812-9229 (Online)**
University of Niš, Faculty of Mechanical Engineering
VOL. 4, NO 1, 2025, PP. ONLINE FIRST

Original scientific paper*

COMPUTATIONAL INVESTIGATION OF FILM COOLING AIRS EJECTED FROM ROW TRENCH AND CYLINDRICAL HOLES

Ehsan Kianpour[1,2], Seyyed Muhammad Hossein Razavi Dehkordi[1,2], Nor Azwadi Che Sidik[3]

[1]Department of Mechanical Engineering, Najafabad Branch, Islamic Azad University, Najafabad, Iran
[2]Aerospace and Energy Conversion Research Center, Najafabad Branch, Islamic Azad University, Najafabad, Iran
[3]Department of Thermo-fluid, Faculty of Mechanical Engineering, University Technology of Malaysia, Skudai, Johor, Malaysia

Abstract. *Gas turbine industries are trying to expand the performance of the gas turbine engine. Using the well-known Brayton cycle, the combustion outlet temperature must be increased to achieve higher efficiency. However, increased turbine inlet temperature creates a harsh environment for downstream combustion components. This requires the design of an efficient cooling technique in this field. In a traditional cooling system, the coolant does not attach well to the surface at higher blow ratios. This requires changing the structure of the cooling holes. A useful way would be to trench the cooling holes in the surface of the end wall of the combustion chamber and align the trenched holes in a row. The major effects of cylindrical and row cooling holes with different alignment angles of 0, ±60 and 90 degrees at BR=1.25 and BR=3.18 on the film cooling effectiveness near the combustion end wall surface are an important issue that needs to be studied in detail. In the present study, the researchers used the FLUENT 6.2.26 package to simulate a 3D model of a Pratt and Whitney gas turbine engine. In this research, RANS model was used to analyze the flow behavior in internal cooling passages. In the combustion simulator, the dilution jets and the cooling stream moved in the flow direction and were also aligned in the transverse direction. Compared to the base case of cooling holes, the use of row holes near the end wall surface increased the film cooling effectiveness from 75% to 100% for different trench cases.*

*Received: October 06, 2024 / Accepted February 25, 2025.
Corresponding author: Ehsan Kianpour
Faculty of Engineering, Najafabad branch, Islamic Azad University, Post code: 8514143131
E-mail: ekianpour@pmc.iaun.ac.ir

Key words: *Gas Turbine Engine, Film-Cooling, Combustor Simulator, Trench Hole, Dilution Hole*

1. INTRODUCTION

Gas turbine industries are trying for higher engine efficiency. The Brayton cycle is key to achieving this goal. In this cycle, to have a higher efficiency of the gas turbine engine, the temperature of the combustion outlet should be increased [1-4]. But such hot flows cause non-uniformities at the end of the combustion chamber and turbine inlet and damage critical parts. Film cooling is the most well-known preservation method. In this technique, a thin layer of low temperature attaches to a surface and protects it from hot flows. To obtain better film cooling performance, the blowing ratio should be increased. Increasing the blowing ratio has a strong effect on heat transfer, especially in the hole region. Due to the importance of this study, an extensive literature review was conducted to obtain basic data. Yuzhen et al. [5] identified the film cooling effectiveness of three different multi-hole designs. In this research, they investigated the effects of cooling row spacing, orifice hole pitch, and hole inclination angle. The results showed that the row spacing ratio affects the cooling performance of the film. Also, better adiabatic cooling performance was obtained by using smaller pitch, especially for multi-hole patterns. Ai and Fletcher [6] and Cun-liang et al. [7] studied a similar case and found that the effectiveness at locations close to the exit of the jets was slightly higher for wide hole spacing than for small hole spacing. Meanwhile, small hole spacing performed better than wide hole spacing at downstream locations due to the interaction of adjacent jets. Kianpour et al [8-9] simulated a realistic large-scale combustion. This model included four different cooling panels with a large number of cooling holes. Two rows of dilution jets can be seen in the second and third cooling panels. The first row had three dilution jets and the second row had two jets. While the first and second panels were flat, the other two panels were angled at 15.8 degrees. In this study, a real large-scale combustion chamber was simulated and high-momentum dilution jets and cooling flow were injected into the mainstream. They presented different geometries of cooling holes. The results showed that temperatures near the wall and between the jets were higher for base cooling, while the central part of the jets was cooler in the trench cases. Using a cascade of turbine blades, the effects of shallow trenched holes (d=0.5D) were investigated by Guan et al. [10]. The results showed that the ratio of coolant momentum and the cooling effectiveness was reduced while at low blowing ratios the performance became better by traditional cooling holes. Using CFD and RNG k−ε turbulence model, Zhang et al. [11,12] investigated the flow and heat transfer behavior in flat plate film cooling of cone-shaped and round-shaped cooling holes. The results showed that with the same tail ratio, the cooling efficiency of the film for conical holes is better than for round holes. Finally, for cone-shaped jets, the ratio of jet blowing to crossflow reaches the optimum condition of 1.0 to obtain the best film cooling effect. In addition, Saumweber and Schulz [13,14], Barigozzi et al. [15], Fawcett et al. [16] and Peng and Jiang [17] showed that better thermal protection is obtained at higher tail ratios. In agreement with the background of the study, several authors motivate the author to conduct this research. The end wall of the combustion chamber can be damaged by the hot gases flowing inside the combustion

simulator, and the enhancement of the cooling effect of the film above these levels is an important issue that has attracts less attention so far. In addition, most of the studies have focused on the use of trenched holes at the leading edge of the turbine blades and in most of them the application of these holes at the end wall combustor is not considered. The alignment angle of trenched cooling holes is an issue that has not been considered in past research. Also, this approach of cooling holes can be utilized by engine designers at the fore side of the turbine vanes. Also, in order to measure the validity of the results, a comparison was made between the data obtained from this research with the project of Vakil and Thole [18] and Stitzel and Thole [19].

2. RESEARCH METHODOLOGY

In the present study, the combustion simulator used was a 3D representation of a Pratt and Whitney gas turbine engine. As seen in Fig. 1, the combustion chamber was a three-dimensional container. The width, height and length of this container were 111.8, 99.1 and 156.9 cm, respectively. The vessel converged from x/L=0.51 and the contraction angle was 15.8 degrees. The cross-sectional areas of the inlet and outlet of the combustion simulator were 1.11 m^2 and 0.62 m^2. The test section consisted of two symmetrical surfaces at the top and bottom of the combustion chamber, but the fluid flowed only through the bottom passage.

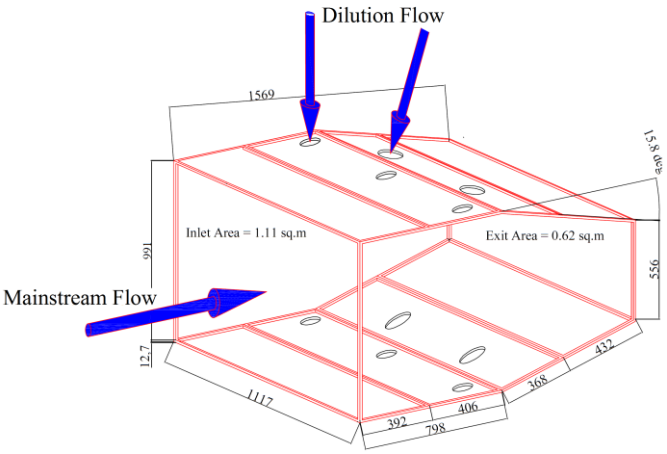

Fig. 1 Schematic view of the combustor simulator

The length of the panels was 39 cm, 41 cm, 37 cm and 43 cm, respectively. In addition, the first two panels are flat and have a constant cross-section. However, the last two panels were inclined at the contraction angle. The panels were 1.27 cm thick and due to their low thermal conductivity (K=0.037 W/mk), adiabatic surface temperature measurements were possible. Two different dilution rows were considered in the second and third panels of cooling panels. The dilution stream is injected vertically into the main stream, while the dilution hole in the third panel is at an angle of 15.8° from the vertical

axis. The first row of dilution jets consisted of three holes and was placed 0.67 m downstream of the combustion simulator inlet. These holes were 8.5 cm in diameter. The second row included two dilution holes and was located 0.23 m downstream of the center of the first row of dilution holes. The diameter of these holes was 12.1 cm. The centerline of the second row was staggered with respect to those of the first row. The length of these cooling holes was 2.5cm and they drilled at an angle of 30deg from the horizontal surface. The film-cooling holes were 0.76cm in diameter. Except the baseline case which introduced, to investigate the effects of cooling holes trenching, different rows of trenched holes with alignment angles of 0, ±60 and 90 degrees with trench depth and width of 0.75D and 1.0D were considered. In addition, the length of the cooling holes after trenching was reduced to 1.36 cm. Also, the coolant blowing ratio was equal to BR=1.25 and BR=3.18. Cartesian coordinate system (x, y and z) was selected. The temperature of the cooling and dilution jets was equal to 295.5K. The main flow temperature was 332K. Fig. 2 shows the observation planes used to measure the film cooling effectiveness distribution. The observation planes 0p, 1p, 2p, and 3p and 0s were placed in pitch-wise and stream-wise direction, respectively. The 0p plane was located at x=35.1 cm. The film cooling momentum distribution along this panel was calculated. The 1p plane was located at the trailing edge of the first row of the dilution jets.

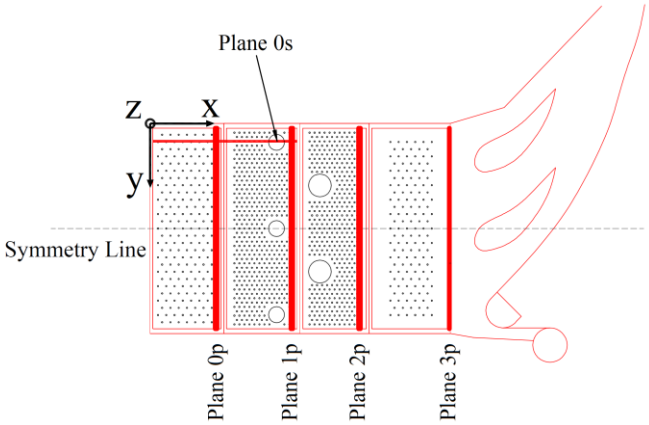

Fig. 2 Location of observation planes

This plane was used to identify the effects of film cooling and dilution jets interaction, as well as the horseshoe, half-wake and counter rotating vortexes effects. The 2p plane was placed at the end edge of the second row of dilution jets. The interaction between the first and second row of dilution jets was determined using a plane. The 3p plane shown in Fig. 2 was at the output of the combustion simulator. It was used to determine the output flow behavior and variable combustion temperature. The 0s plane was placed in the center of the first row of the dilution jet. The importance of this aircraft was to identify the stream-wise behavior of the first-row dilution jets. About 8×10^6 tetrahedral meshes was selected. The meshes were denser around the cooling and dilution holes as well as the wall surfaces. According to the blowing ratio considered at the inlet of the control volume, the boundary conditions of the inlet mass flow were considered at the inlet. To

limit the interaction area between the fluid and the combustion wall, no-slip boundary conditions and wall boundary conditions were considered. In addition, two different boundary conditions of uniform flow and pressure output were selected at the inlet and outlet of combustion, respectively. In general, according to the symmetry of the Pratt and Whitney gas turbine engine combustion chamber, symmetry boundary conditions were used. The numerical method considered a transient and incompressible turbulent flow using the k-ε turbulent model of the Navier-Stokes equations, which is expressed as follows:

Continuity equation

$$\frac{\partial}{\partial t}\left(\rho u_i\right)+\frac{\partial}{\partial x_j}=\left(\rho u_i u_j\right)=-\frac{\partial \mathrm{P}}{\partial x_i}+\frac{\partial \tau_{ij}}{\partial x_i}+\rho g_i+\vec{F}_1 \tag{1}$$

Momentum equation

$$\frac{\partial \rho}{\partial t}+\frac{\partial \rho}{\partial x}\frac{dx}{dt}+\frac{\partial \rho}{\partial y}\frac{dy}{dt}+\frac{\partial \rho}{\partial z}\frac{dz}{dt}=-\rho\left(\nabla.V\right) \tag{2}$$

Energy equation

$$\frac{\partial}{\partial t}\left(\rho E\right)+\frac{\partial}{\partial x_i}=\left(u_i\left(\rho E+P\right)\right)=\frac{\partial}{\partial x_i}\left(K_{eff}\frac{\partial T}{\partial x_i}-\sum\nolimits_j h_j J_j+u_i\left(\tau_{ij}\right)_{erf}\right)+S_h \tag{3}$$

k–ε equation

$$\frac{\partial}{\partial t}\left(\rho k\right)+\frac{\partial}{\partial x_i}\left(\rho k u_i\right)=\frac{\partial}{\partial x_i}\left(\mu+\frac{\mu_t}{\sigma k}\frac{\partial k}{\partial x_j}\right)+P_k-\rho\varepsilon \tag{4}$$

$$\frac{\partial}{\partial t}\left(\rho\varepsilon\right)+\frac{\partial}{\partial x_i}\left(\rho\varepsilon u_i\right)=\frac{\partial}{\partial x_j}\left(\left(\mu+\frac{\mu_t}{\sigma\varepsilon}\right)\frac{\partial\varepsilon}{\partial x_j}\right)+C_{1\varepsilon}\frac{\varepsilon}{k}P_k-C_{2\varepsilon}^{*}\rho\frac{\varepsilon^2}{k} \tag{5}$$

To check the convergence limit, the control volume mass residue was estimated and the maximum value was used. For this research, the convergence criterion of 10^{-4} was chosen. The following equation was used to determine the effectiveness of film cooling:

$$\eta=\frac{T-T_\infty}{T_c-T_\infty} \tag{6}$$

3. RESULTS AND DISCUSSIONS

The findings of the present research were compared with the experimental results collected by Vakil and Thole [18] and the numerical findings collected by Stitzel and Thole [19]. The film cooling effect was compared in 1p and 2p plane at y/W=0.4. Deviation between current research results and benchmarks was calculated with the following equation. The deviation compared to Vakil and Thole [18] measurements and Stitzel and Thole [19] estimates for plane 1p was 9.76% and 8.34% compared to Ref [18] and Ref [19] for plane 2p (Fig. 3).

$$\%Diff = \frac{\sum_{i=1}^{n} \frac{x_i - x_{i,benchmark}}{x_{i,benchmark}}}{n} \times 100 \quad (7)$$

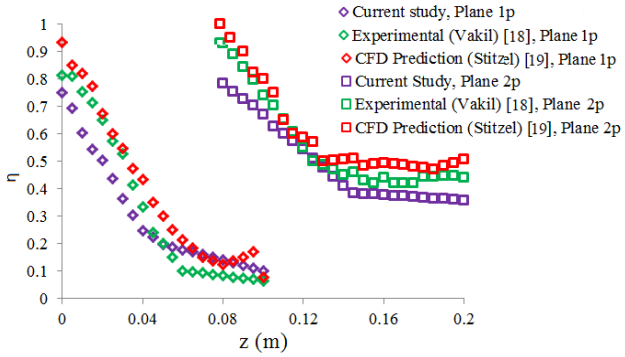

Fig. 3 The film cooling effectiveness comparison of planes 1p and 2p along y/W=0.4

Much of the film cooling effectiveness data in this study were collected on the assumption that symmetry could be applied within the combustor simulator. Fig. 4 shows a distribution of vertical film cooling effectiveness taken at the intersection of panels 1p and 0s extending approximately over 10% of the total inlet height at high lowing ratios of 1.25 and 3.18. The trailing edge footprints of both dilution jets can be seen in the figure. According to Fig. 4, since the cooling effect of the film reaches η=0.905 in the vicinity of the combustion end wall surface, the performance of this type of trenched holes was significantly more efficient than others. It should be noted that there is a slight difference between the trenched holes with +60° and 90° alignment angles (about 3%), which may be caused by the coolant-dilution interaction at this point. As the vertical distance from the end wall surface became larger, the cooling performance decreased continuously for both baseline and trenched holes with 60° and 90° alignment angle. However, the film cooling performance of the trenched holes with the alignment angle of +60 degrees decreased with the line slope of -0.324, which was lower than the other types. For trenched holes with alignment angles of -60 and 90°, the cooling effectiveness increased so that it provided higher cooling than the other configurations (η=0.919) but then decreased at greater distances.

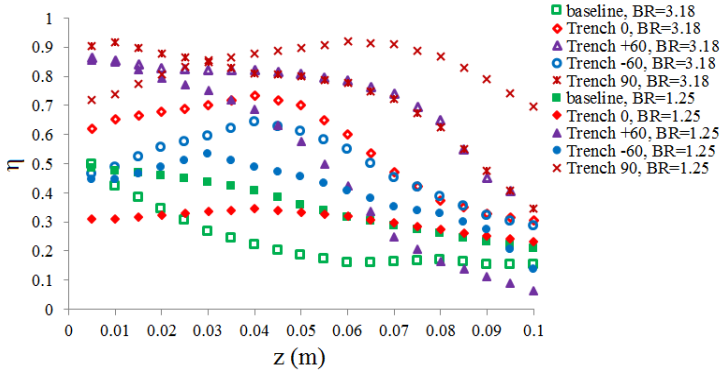

Fig. 4 Film cooling effectiveness distribution at the intersection point of planes 1p and 0s

Fig. 5 shows the film cooling effectiveness of the 0p plane at the blowing ratio of BR=1.25 and BR=3.18.

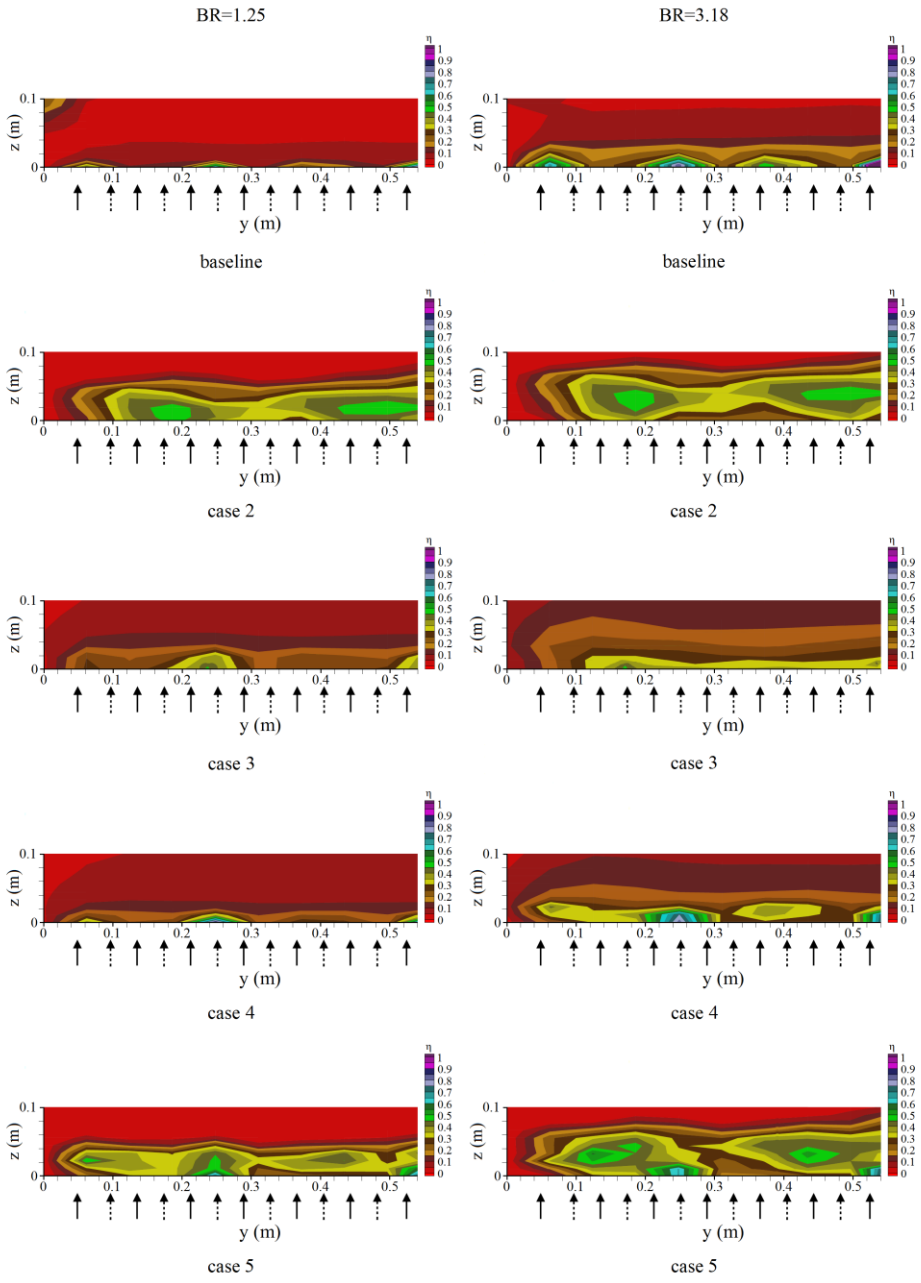

Fig. 5 Film cooling effectiveness of plane 0p

The observation plane was located at x/L=0.24, which was two film cooling hole diameters (2d) downstream of the trailing edge of the last row of cooling holes in panel

one. Since the liner panels were made to represent a staggered film-cooling pattern, the dashed arrows denote the upstream film-cooling holes, whereas the solid arrows show the downstream holes. The jets closest to the observation plane (the last row on panel 1) had their coolest region near the wall with a secondary cool region directly above it. This secondary cool region was a remnant of the upstream film-cooling jet that exited from the aligned cooling hole. This effect was negligible in the upstream holes because the two regions were combined in this location. No significant difference was observed between the base case and trenched holes with an alignment angle of 0 degree for the observation plane of 0p and at low blowing ratios. We suggest to produce a cold protected layer near the surface of the end wall, which is made possible by the use of a trenched hole. However, the hotter region ($0<\eta<0.05$) was observed at a greater distance from the end wall surface ($5cm<z<10cm$), especially in the configuration of trenched holes with the alignment angles of 90° and ±60°. The significant difference between these lines is the thickness of the cooling film layers. When BR=1.25, the thickness of the film cooling layer for the trenched case with a 90° alignment angle reaches the maximum z=4cm, which is 4% of the total height of the combustion inlet. But when BR=3.18, the maximum z=7.1cm is 7.2% of the input height. It is obvious that the penetration depth is greater when BR=3.18 than when BR=1.25. However, a thicker film cooling layer is not always desirable for higher momentum flux. Compared to the temperature distribution contour of trenched holes with 90° alignment angle and blow ratio BR=1.25, the temperature level near the end wall surface was higher at BR=3.18 for the trenched case with alignment angle of 90° and in the position of $31cm<y<36cm$.

Film cooling effectiveness in plane 1p was taken directly downstream of the first row of dilution jets. This particular hole is located in the center of the combustion simulator. The thermal field results are shown in Fig. 6. The results show that the center of the dilution jet is reasonably rotated at the corners of this viewing plane as the dilution jet rises. Note that the jet spread is slightly higher there for y=10cm and y=50cm. This may be due to the interaction of the jet with its upper row. Also, unlike the baseline, it is slightly warmer ($0<\eta<0.05$) for the trenched case with 90° and +60° alignment angles at $14cm<y<52cm$ and $8cm<z<10cm$. For trenched holes with an alignment angle of -60°, the hot zone becomes smaller ($18cm<y<50cm$). However, compared to others, these types of trench holes are more efficient in the vicinity of the end wall surfaces. Also, the results show the effect of increasing the cooling motion flux compared to the interaction with the main flow. Note that when the film cooling increased significantly, the dilution jet injection remained constant. Fig. 6 shows slightly higher near-wall levels for the trenched cases than the baseline, especially for trenched holes with 90° and ±60° alignment angles. However, no major improvement in cooling along the liner wall was observed. It was just downstream of the dilution jet and near the corners that the thermal field lines indicated that the film coolant was bubbling as the dilution jet moved upward. In addition, the temperature was slightly higher for trenched holes with 90° and +60° alignment angle at $18cm<y<28cm$ and $38cm<y<50cm$ ($0<\eta<0.05$). Of course, the hot zone is extended from y=18cm to y=50cm for trenched holes with a level angle of -60 degrees. For trenched holes with alignment angles of +90° and +60°, the area in the range of $14cm<y<52cm$ and $8cm<z<10cm$ is visible in the tail ratio BR=1.25.

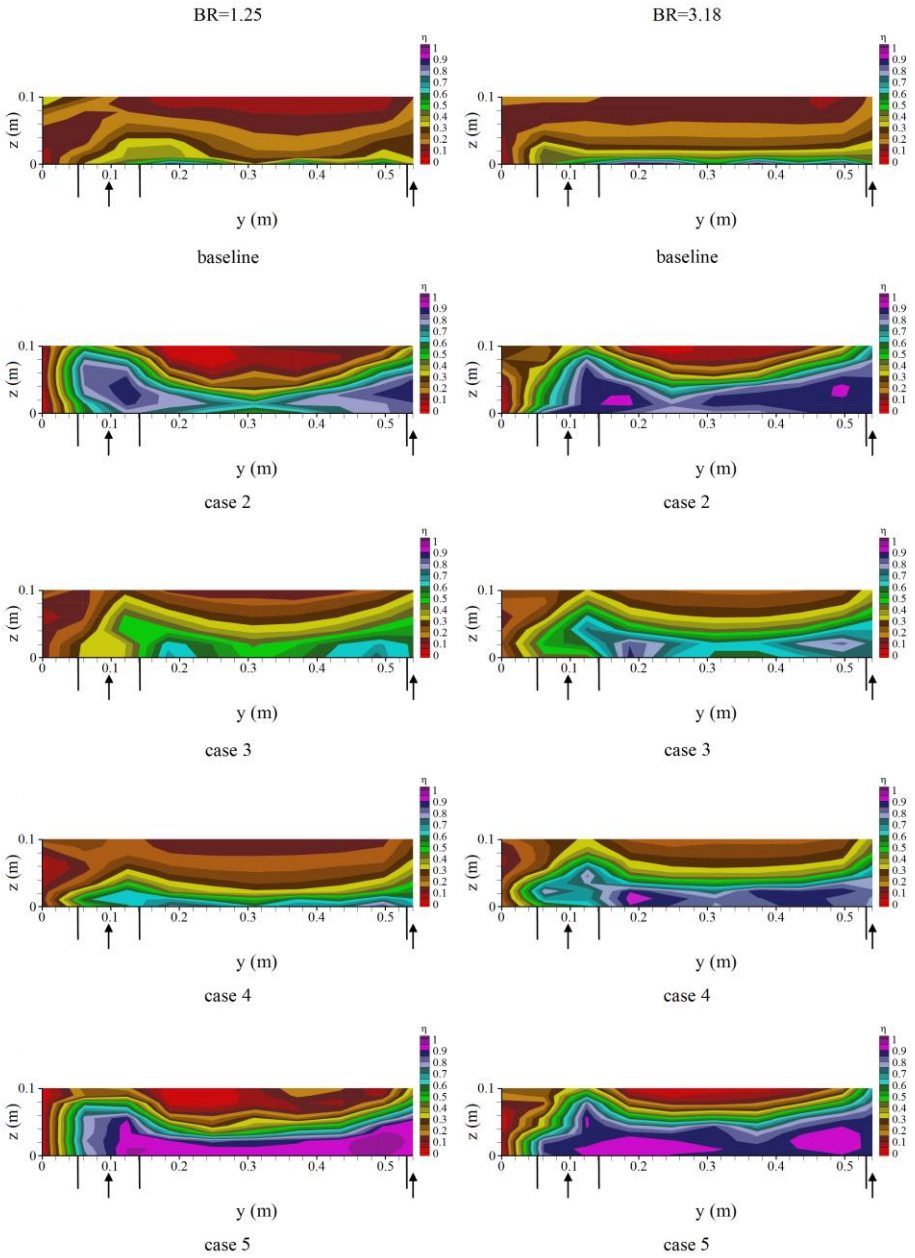

Fig. 6 Film cooling effectiveness for plane 1p

Fig. 7 shows the cooling performance curves of the film on the 2p plane at BR=1.25 and BR=3.18 located at one dilution hole diameter (1D2) downstream of the end edge of a two-dilution hole.

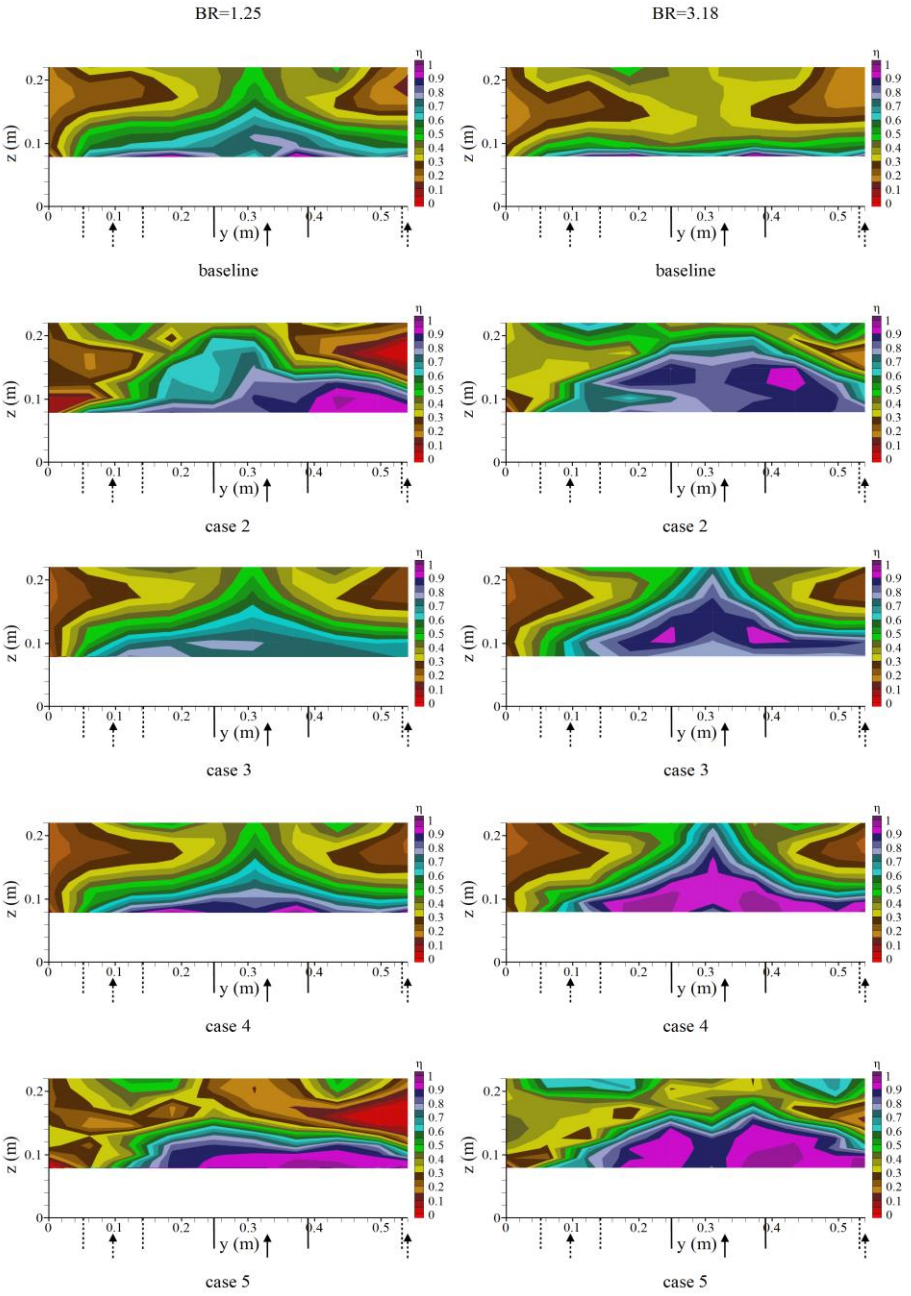

Fig. 7 The film cooling effectiveness comparison of planes 1p and 2p along y/W=0.4

As can be seen on the right side of the lines, the mushroom shaped temperature profiles were mixed and a warmer region emerged near the middle opening. It is likely

that the hot region is formed as a result of the flow of warmer unmixed fluid around the stagnation region caused by the impingement of opposing dilution jets in the first row. The high temperature region observed along y=52cm and height z=15cm was the trace of hot fluid trapped in the downstream swirl region of the first row of dilution jets. This area was warmer for the row of trenched holes with alignment angles of 90° and ±60° ($\eta<0.05$). At low blowing ratio and at the midspan, the remnants of trapped fluid behind the first-row dilution jet show core temperatures ranging between $0.25<\eta<0.3$ for the baseline case and row trenched cooling holes with alignment angles 0f 0° and -60° and $0<\eta<0.05$ for the row trenched cooling holes with alignment angles of 90° and +60°. At high blow ratio, the injection of coolant into the main flow is the main difference between the lines. Right at the trailing edge of the second row of dilution jets and at higher tail ratios, the trenched holes created a protective layer (10cm<y<50cm) on the critical surfaces that was more efficient than the baseline. This was especially noticeable for trenched holes with alignment angles of 0, +60 and 90 degrees ($0.9 < \eta < 1.0$). the highest film cooling layer at low blowing ratio of BR=1.25 reached z=14cm at the mid pitch (which was 14% of the combustor inlet height) at BR=3.18, this layer reached at z=18cm for the trenched holes with alignment angles of +60 and 90 degrees. For the trenched holes with alignment angle of 0 degree, the maximum height of the layer was 20 cm, equal to 20% of the combustor inlet height. This gave the highest cooling layer among all the cases.

Fig. 8 shows the distribution of the film cooling effectiveness for the 3p plane and shows the flow behavior at the end of the combustion simulator where x/L is equal to 1.0. The highest fluctuations in flow temperature were observed near a (32cm<z<38cm) for trenched holes with horizontal angles of +90° and +60°. For these two types of row cooling holes, the mushroom-shaped temperature profiles are mixed together and a warmer region is formed in the corners. This heat flows from the unmixed heater around the stagnation zone created by the interaction of the dilution jets in the second row. For the configuration of trenched holes with a 90° alignment angle, the peak region was slightly higher than where the direction of the velocity vectors changed in the reverse flow region. For base and trenched holes with 0° alignment angle, the trailing edge of the jet mixes with the main flow. The jet temperature component in terms of flow indicates the existence of a slow flow at the end of the combustion chamber. A secondary cool region is seen directly above the (0cm<y<16cm) and (50cm<y<54cm) lines, which is the remnant of the upstream dilution jet in the first row. This secondary cooling zone is extreme for trenched cooling holes with 90° and +60° alignment angles. At the midspan, the remnants of trapped fluid downstream the second-row dilution jet show core temperature ranging between $0.45<\eta<0.65$. At high blowing ratio of BR=3.18.

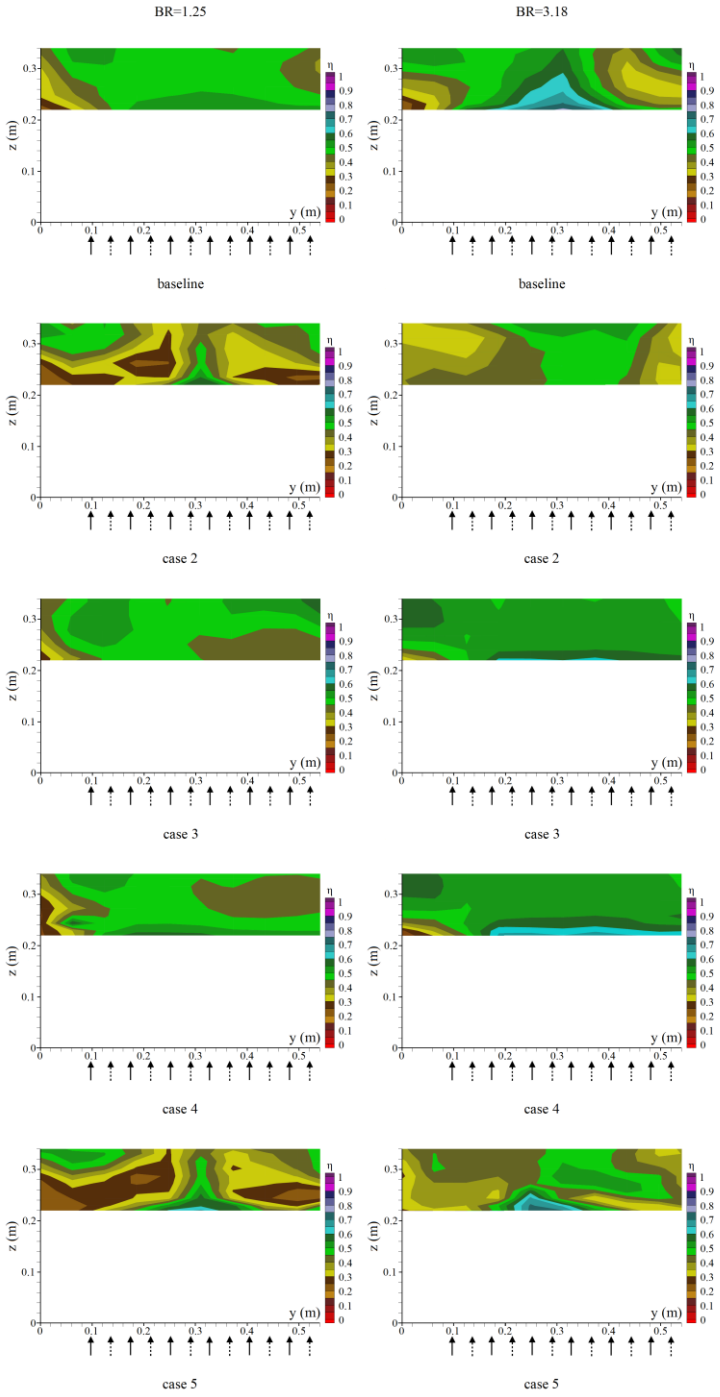

Fig. 8 Film cooling effectiveness for plane 1p

4. CONCLUSIONS

In this research, a numerical study was conducted in order to better understand the film cooling effectiveness and the effects of trenched cooling holes with different alignment angles of 0°, 90° and ±60° from the combustion output of a gas turbine engine. Optimal design of the cooling holes helps maximize cooling effectiveness along the combustion end wall surface and prevents premature wear in this area. A 3D representation of a gas turbine engine was simulated to analyze the effects of row cooling holes. The combustor simulator combined the effects of two rows of stream-wise staggered and span-wise aligned dilution jets. The FLUENT software package and RNG k-ε turbulence model were used to perform calculations on thermal fields in a combustion simulator under two different blowing ratios of 1.25 and 3.18. Compared to the baseline method, in the trenched case, the coolant stayed closer to the end wall surface and did not allow main entrainment. It also provided significant lateral spreading and stronger coverage. As a rule, trenched holes performed much more efficiently at both blowing ratios, especially at BR=3.18. All types of row cooling holes appeared to increase the effectiveness of film cooling. Film cooling was also investigated at high blowing ratios and observation planes of 0p and 2p, using trenched holes with an alignment angle of 60°. However, for the 1p plane, i.e., at the trailing edge of the second cooling panel, the row trenched holes with an alignment angle of 90° increased the film cooling effectiveness by 75%, which is much higher than the other configurations. In addition, apparently the highest effectiveness was observed downstream of the first cooling panel as a result of the use of trenched cooling holes with a 0° alignment angle. In the case of the jet advancing downstream, different cooling hole geometries showed similar behavior at the end of the combustion chamber. Comparisons between the data computationally predicted and those collected by Vakil and Thole [18] and Stitzel and Thole [19] indicated the existence of similarities and differences. The predicted thermal field data showed an under-predicted measurement for the current study in contrast to the experimental findings. Based on the results of this research, the following recommendations are provided for future research in this field. It was not clear which trench holes with different alignment angles had stronger effects on film cooling effectiveness. Because the behavior of the holes was quite different at low and high tail ratios and even from one viewing plane to another, it is therefore highly recommended to observe the combined effects of row cooling holes.

REFERENCES

1. Zhang, G., Zhu, R., Xie, G., Li, S., Sunden, B., 2022, Op*timization of cooling structures in gas turbines: A review*, Chinese Journal of Aeronautics, 35(6), pp. 18-46.
2. Zhang, J., Zhang, S., Wang, C., Tan, X., 2020, *Recent advances in film cooling enhancement: A review*, Chinese Journal of Aeronautics, 33(4), pp. 1119-1136.
3. Unnikrishnan, U., Yang, V., 2022, *A review of cooling technologies for high temperature rotating components in gas turbine*, Propulsion and Power Research, 11(3), pp. 293-310.
4. Ren, J., Li, X., Guo, X., Wang, S., Xu, H., 2022, *Development trends in high-efficiency gas turbine cooling methods*, Tsinghua Science and Technology, 62(4), pp. 794-801.
5. Yuzhen, L., Bo, S., Bin, L., Gaoen, L., 2006, *Measured Film Cooling Effectiveness of Three Multihole Patterns*, Journal of Heat Transfer, 13(1), pp. 11-23.
6. Ai, W., Fletcher, T.H., 2012, *Computational Analysis of Conjugate Heat Transfer and Particulate Deposition on a High Pressure Turbine Vane*, Journal of Turbomachinery, 134(4), pp. 11-23.
7. Liang, S., Dong, R.L., Xu, W.W., Wei, Y.Q., 2024, *Numerical Analysis of Film Cooling Flow Dynamics and Thermodynamics for Perfect and Imperfect Cooling Holes*, Journal of Applied Fluid Mechanics, 17(6), pp. 1322-1338.
8. Che Sidik, N.A., Kianpour, E., 2014, *The Effect of Blowing Ratio on Film Cooling Effectiveness Using Cylindrical and Row Trenched Cooling Holes with Alignment Angle of 90 Degrees*, Mathematical Problems in Engineering, 2014(1), pp. 470576.
9. Kianpour, E., Che Sidik, N.A., Abdul Wahid, M., 2013, *Cylindrical and Row Trenched Cooling Holes with Alignment Angle of 90o at Different Blowing Ratios*, CFD Letters, 5(4), pp. 165-173.
10. Guan, P., Ai, Y.T., Fei, C.W., 2019, *An enhanced flow-thermo-structural modeling and validation for the integrated analysis of a film cooling nozzle guide vane*, Journal of Energies, 12(4), pp. 2775.
11. Zhang, B.L., Zhu, H.R., Yao, C.Y., Liu, C.L., Zhang, Z., 2021, *Investigation on film cooling and aerodynamic performance of blade tip with tangential jet cooling scheme at transonic flow*, Aerospace Science and Technology, 118(1), pp. 107067.
12. Zhang, B., Chen, Y.X., Wang, Z.G., Li, J.Q., Ji, H.H., 2021, *Influence of Mach number of main flow on film cooling characteristics under supersonic condition*, Journal of Symmetry, 13(1), pp. 127.
13. Saumweber, C., Schulz, A., 2012, *Free-stream effects on the cooling performance of cylindrical and fan-shaped cooling holes*, Journal of Turbomachinery, 134(6), pp. 061007.
14. Saumweber, C., Schulz, A., 2012, *Effect of geometry variations on the cooling performance of fan-shaped cooling holes*, Journal of Turbomachinery, 134(6), pp. 061008.
15. Barigozzi, G., Mosconi, S., Perdichizzi, A., Ravelli, S., 2017, *The effect of hot streaks on a high-pressure turbine vane cascade with showerhead film cooling*, International Journal of Turbomachinery, Propulsion and Power, 2(3), pp. 15.
16. Fawcett, R.J., Wheeler, A.P.S., He, L., Taylor, R., 2013, *Experimental investigation into the impact of crossflow on the coherent unsteadiness within film cooling flows*, International Journal of Numerical Methods for Heat & Fluid Flow, 40, pp. 32-42.
17. Ni, H., Peng, W., Wang, J., Zhu, Y., Jiang, P., 2021, *A numerical study of supersonic film cooling with discrete holes*, In International Conference on Nuclear Engineering, 85253(1), pp. V002T07A019.
18. Vakil, S.S., Thole, K.A., 2005, *Flow and Thermal Field Measurements in a Combustor Simulator Relevant to a Gas Turbine Aero engine*, Journal of Engineering for Gas Turbines and Power, 127(2), pp. 11-23.
19. Stitzel, S., Thole, K.A., 2004, Flow field computations of combustor-turbine interactions relevant to a gas turbine engine, Journal of Turbomachinery, 126, pp. 175-183.